12 MW

Final report

Hasager, Charlotte Bay; Pena Diaz, Alfredo; Mikkelsen, Torben; Gryning, Sven-Erik; Courtney, Michael; Sørensen, Paul B.

Publication date:
2009

Document Version
Publisher's PDF, also known as Version of record

12MW: final report

Risø-R-Report

Charlotte Hasager, Alfredo Peña, Torben Mikkelsen, Sven-Erik Gryning, Mike Courtney, Paul B. Sørensen (DONG energy)
Risø-R-1690(EN)
June 2009

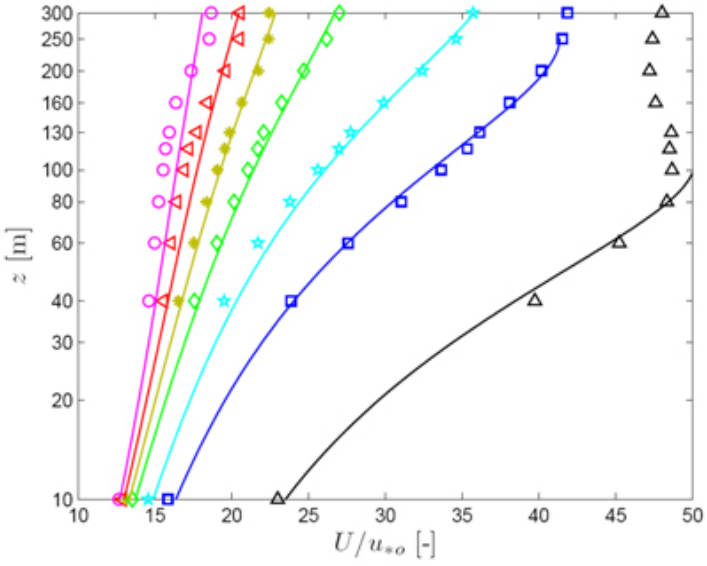

Risø DTU
National Laboratory for Sustainable Energy

Author: Charlotte Hasager, Alfredo Peña, Torben Mikkelsen, Sven-Erik Gryning, Mike Courtney, Paul B. Sørensen (DONG energy)
Title: 12MW: final report
Division: Wind Energy Division

Risø-R-1690(EN)
June 2009

Abstract (max. 2000 char.):

'12MW: final report' is for the project with the full title '12 MW wind turbines: the scientific basis for their operation at 70 to 270 m height offshore' that had the goal to experimentally investigate the wind and turbulence characteristics between 70 and 270 m above sea level and thereby establish the scientific basis relevant for the next generation of huge 12 MW wind turbines operating offshore. The project started 1st October 2005 and ended 31st March 2009. Firstly was conducted a 6-month experiment at the Horns Rev offshore wind farm deploying a lidar and a sodar on the transformer platform. The observed data were successfully compared to offshore mast data and the wind profile was extended 100 m above previous levels observed in this offshore environment. The wind and turbulence was observed up to 160m above mean sea level. A new normalization was introduced to group the wind profiles into stability groups with variable roughness. Secondly two experiments were conducted at Høvsøre at the North Sea coast in Jutland. Again the wind profile was extended far beyond previous observed levels, up to 300 m above ground. The analysis showed that the profiles extended far beyond the surface layer and therefore surface layer scale alone could not described the profiles well. In addition the boundary layer height has to be used for the scaling. The boundary layer height was observed by an aerosol lidar at Høvsøre. The results are published widely, please see the list of publications.

ISSN 0106-2840
ISBN 978-87-550-3746-5

Contract no.: 2104-05-0013

Group's own reg. no.:
(1130314-01)

Sponsorship:
Danish Strategic Research Council, EnMi

Cover : Mean wind speed profiles observed at Høvsøre, Risø DTU combining mast and lidar data up to 300 m above ground. The different curves show very unstable, unstable, slightly unstable, near-neutral, slightly stable, stable and very stable conditions (markers) and fitted profiles using roughness and boundary layer height for scaling. Alfredo Peña.

Pages: 39
Tables: 6
References: 15

Information Service Department
Risø National Laboratory for Sustainable Energy
Technical University of Denmark
P.O.Box 49
DK-4000 Roskilde
Denmark
Telephone +45 46774004
bibl@risoe.dk
Fax +45 46774013
www.risoe.dtu.dk

Contents

Preface

'12MW: final report' is for the project with the full title '**12MW** wind turbines: the scientific basis for their operation at 70 to 270 m height offshore' that had the goal to experimentally investigate the wind and turbulence characteristics between 70 and 270 m above sea level and thereby establish the scientific basis relevant for the next generation of huge 12 MW wind turbines operating offshore. The project started 1st October 2005 and ended 31st March 2009.

Acknowledgments: The Strategic Research Council is very thankfully acknowledged for the support of the 12MW project Sagsnr. 2104-05-0013. Our close collaboration with DONG energy is greatly acknowledged and the collaboration with the Risø DTU research technicians Per Hansen, Anders Ramsing Vestergaard og Bjarne Sønderskov is also greatly acknowledged.

1 Introduction on the 12MW project

The project '**12MW** wind turbines: the scientific basis for their operation at 70 to 270 m height offshore' was funded by the Danish Council for Strategic Research during the years 2006 to 2009. The project was called '**12MW**'. In the first year an experiment was carried out at Horns Rev offshore wind farm. The partners Risø DTU and DONG energy cooperated closely in the project. The results from the Horns Rev experiment are described in Hasager et al. 2007 http://www.risoe.dk/rispubl/reports/ris-r-1506.pdf. In the second and third year an experiment was carried out at Høvsøre in Jutland, and the major results are described in the present report.

The report contains the introduction (chapter 1); the results from the Høvsøre experiment (chapter 2); note on turbulence observed from lidar (chapter 3); information on the database and access (chapter 4); complete list of publications from the project (chapter 5); final conclusion and perspective (chapter 6).

1.1 Background

Wind turbine dimensions have evolved rapidly (see Fig. 1.1). Thus the height in the atmospheric boundary layer of wind turbine operation is increasing (Table 1.1). At Høvsøre National Test Station at Risø DTU wind turbines up to 8 MW can be tested but even larger turbines are in preparation up to 12 MW. This development puts a strong demand on our understanding of the atmospheric flow and turbulence characteristics at very high heights.

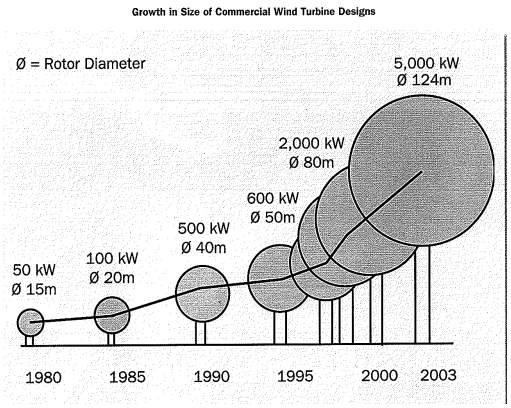

Figure 1.1 Dimensions of wind turbines through time.

Table 1.1 Dimensions of multi-MW wind turbines.

Turbine	Hub-height	Rotor diameter	Lower tip	Upper tip
2 MW	70 m	80 m	30 m	110 m
5 MW	110 m	124 m	48 m	172 m
8 MW	140 m	160 m	60 m	220 m
12 MW	170 m	190 m	75 m	265 m

Small turbines operate in the lower part of the atmospheric boundary layer. Here the logarithmic wind profile is valid and turbulence statistics are well known. At higher levels winds are largely unknown due to severe practical offshore measurement difficulties.

The challenge was therefore to improve our knowledge on offshore wind and turbulence characteristics for the next generation of multi-MW wind turbines that will come to operate at heights ranging from 70 to 270 m above sea level. Offshore winds and turbulence were observed at these heights using lidar. The strategic aim is to supply Danish wind industry relevant results.

1.2 Goal

The goal of the project was to experimentally investigate the wind and turbulence characteristics between 70 and 270 m above sea level and thereby establish the scientific basis relevant for the next generation of huge 12 MW wind turbines operating offshore. This was done using state of the art wind remote sensing measurement techniques for data collection at an offshore wind farm site in Denmark.

Innovation

The innovations were establishment of new reference data and new wind and turbulence profiles at 70 to 270 m, unique experimental set-up at offshore wind farm in rough environment, advanced signal processing of state of the art remote sensing wind observations and estimating the mixing layer height from remote sensing observations.

Objective

To establish new wind and turbulence design models for the next generation of 12 MW turbines operating in the offshore marine environment from 70 to 270 m's height. The wind and turbulence profile was evaluated from observations from lidar, sodar, aerosol lidar (ceilometers) and radiosonde.

1.3 Technical basis

To measure winds and turbulence between 70 and 270 m is a true challenge. A conventional meteorological mast for these heights over sea is utterly expensive. Remote sensing technologies have consequently become an attractive option, given their data are scientifically interpreted. New remote sensing technologies such as wind lidar for accurate wind observations at high levels have become available. Advantages of these instruments are that they, at reasonably cost, observe winds and turbulence up to 300 m from their local position. Mixed layer height (an important scaling parameter) was monitored from ceilometers (aerosol lidar) and radiosoundings.

1.4 Scientific issues and state of the art

The major scientific issue is to experimentally evaluate new mathematical models for prediction of the winds and turbulence characteristics at high levels above the sea. This is crucial for obtaining a detailed design-knowledge for the next-generation multi-MW wind turbines. The turbine structures will be enormous and the wind shear between tip of wings significant. Wind climate at hub-height and across the rotor diameter is unknown. To our knowledge, it had not been measured anywhere. Verified models were not available.

Wind and turbulence data was obtained at high levels in the marine boundary layer in this project. The planned experimental set-up relied on proven state of the art remote sensing technology applied to operation in a harsh environment. The Horns Rev offshore wind farm offered unique opportunity for safe mounting of the instruments and excellent meteorological observations for comparison in the lower part of the atmosphere.

The '12MW'-project quantified winds and turbulence at 70 to 270 m height. Such a project requires guidance from a professional experimental research team because it would have been beyond capabilities of wind turbine manufacturers and wind energy developers to deploy the new remote sensing sensors in an experimental campaign, to apply advanced signal processing to the data stream, to retrieve and finally to evaluate theoretical models on winds and turbulence. The '12MW' project was basis foundation research with strategic aim for the next generation of multi-MW turbines.

1.5 Methodology

The marine winds and turbulence high above sea surface were observed as:

- wind speed and direction at various levels (*U(z), dir*)
- turbulence parameters at various levels (u_*, σ_u, σ_v , σ_u)
- air temperature at various levels (T_a)
- heat flux observations at one level (H)
- mixing layer height (z_i)

The methodology was to measure the above parameters with the highest possible accuracy for six months offshore at the Horns Rev wind farm (year 2006). The following instruments were used for the vertical dimension:

- Three tall meteorological masts with sonic and cup anemometers, thermometers (up to 70 m)
- lidar (Zephir) (up to 160 m)
- sodar (up to 270 m),

The methodology was later also applied to Høvsøre (years 2007-2008). The following instruments were used for the vertical dimension:

- Two tall meteorological masts with sonic and cup anemometers, thermometers (up to 160 m)
- Lidar (WindCube) (up to 300 m),
- Ceilometer (up to 3.000 m)
- Radiosounding (up to 3.000 m)

2 Experiment Høvsøre with results

Alfredo Peña

2.1 Site description

The measurements over land (the first part of the experiment was carried out over the North Sea at the Horns Rev wind farm) were performed at the National Test Station for Wind Turbines located at Høvsøre, Denmark. This is a rural area near the west cost of Jutland, very close to the North Sea, as illustrated in Fig. 2.1. From the view of the tall meteorological mast, there is a wide upwind area where the terrain is flat and homogeneous and in which the wind is neither influenced by the water, west and south of the mast, nor by the wind turbines north of the mast (Jørgensen *et al.* 2008). This nearly 100° wide sector, 30°−125°, was selected for the analysis.

Two different campaigns using two different WindCube wind lidars (from the company Leosphere) were performed at Høvsøre. The first was carried out during the period 22nd of December 2007 to 22nd of February 2008 (hereafter winter campaign). A second campaign (hereafter summer campaign) was performed during the period 6th of July 2008 to 26th of October 2008.

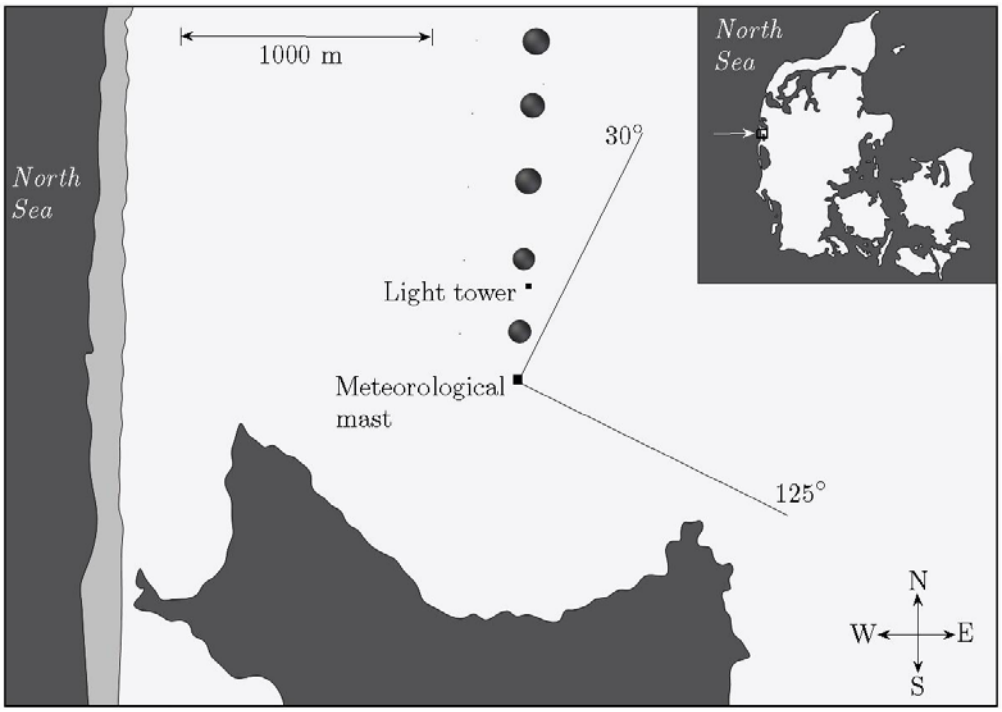

Figure 2.1 National Test Station for Wind Turbines at Høvsøre, Denmark. The positions of the meteorological masts (56°26'26''N, 8°9'3''E), light tower (small rectangle), and five wind turbines (in circles) are indicated. At the top-right corner, the location of Høvsøre in Denmark is shown. The dark color indicates water and the white/light gray areas indicate land surfaces.

The meteorological mast is instrumented with Risø cup anemometers at 10, 40, 60, 80, 100, and 116 m, wind vanes at 10, 60, and 160 m, and Metek USA-1 sonic anemometers at 10, 20, 40, 60, 80, and 100 m. In addition, equivalent cup and sonic anemometers are installed at 160 m on the light tower 400 m north of the meteorological mast.

2.2 The WindCube wind lidar

The WindCube lidar, produced by the French company Leosphere, is a ground-based remote sensing wind lidar used for wind speed measurements and profiling for wind energy applications. As the ZephIR wind lidar (described in Hasager *et al*. 2007 and Peña *et al*. 2009a, and used in the first phase of this project), the WindCube measures the Doppler-shifted frequency Δf of the backscattered light from aerosols in the atmosphere when illuminated by a source laser. Thus, if the aerosols are moving relative to the lidar, the instrument is able to measure the radial velocity, line-of-sight or along-beam velocity, v_r, of the particles relative to the lidar (see Fig. 2.2):

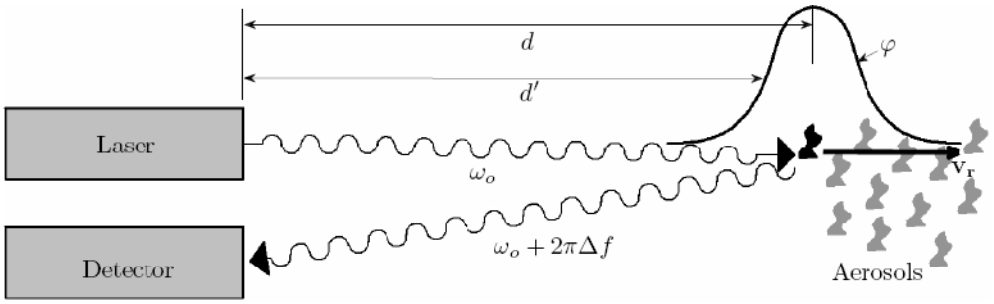

Figure 2.2 The principle of measurement of the WindCube. Light is emitted from a laser source illuminating a target at a distance d. The backscatter light experiences a Doppler shift in the frequency Δf. Contributions of targets at distances d' are weighted in the beam direction by a function φ.

$$v_r = \frac{\lambda_l \Delta f}{2} \tag{2.1}$$

where λ_l is the laser wavelength. Scattering from any moving target at a distance d' is weighted in the along-beam direction by a function φ.

The WindCube is a pulsed coherent monostatic wind lidar operating at $\lambda_l = 1.54\ \mu$m and uses the time of flight to discriminate between returns from different ranges or heights. The along-beam weighting function is approximated by

$$\varphi = \begin{cases} \dfrac{l_w - |d' - d|}{l_w^2} & \text{for } |d' - d| < l_w \\ 0 & \text{elsewhere} \end{cases} \tag{2.2}$$

where l_w is the WindCube's full width at half maximum (FWHM) length, which depends on the system's pulse length, $\tau = 200$ ns, and the speed of light, c_l,

$$l_w = \frac{c_l \tau}{2}. \tag{2.3}$$

Therefore, the FWHM length is constant and equal to 30 m for the WindCube, in contrast to the continuous wave (CW) wind lidars, in which the FWHM increases quadratically with focusing height. The corresponding weighting function of the WindCube is illustrated in Fig. 2.3 for three different focal distances and compared to a typical CW wind lidar. Particles "out of focus" at distances above 100 m from

the ground are expected to have a much higher backscatter contribution for the CW unit than for the pulsed WindCube.

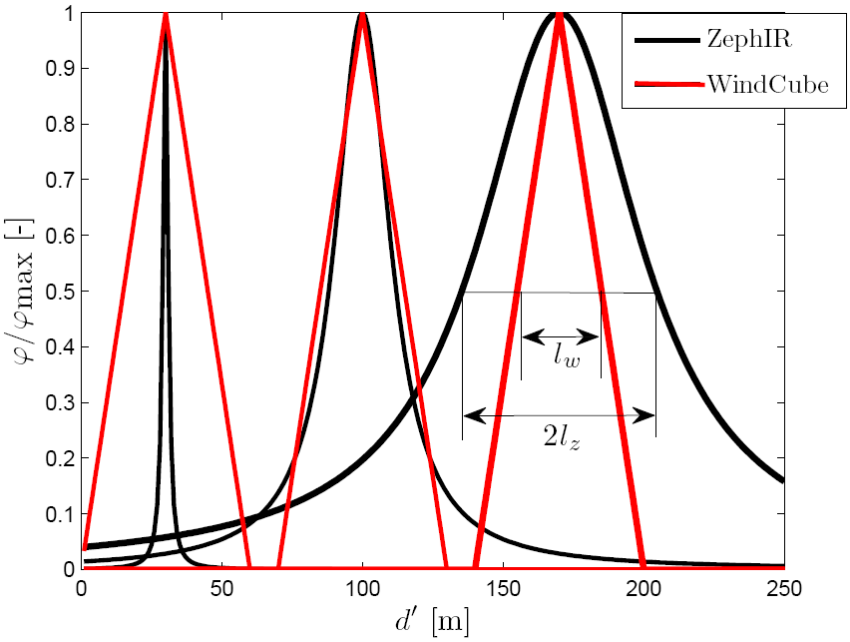

Figure 2.3 Normalized along-beam weighting function, φ/φ_{max}, for three focal distances (30, 100 and 170 m), for the CW ZephIR and WindCube lidars. The FWHM for both systems is also shown.

In the WindCube system, a stream of pulses (5000-10000) is sent and the detector records the backscatter light in a number of range gates for fixed time delays. For each gate, the time series of each pulse is Fourier transformed to a block average power spectrum. Leosphere developed a mathematical model to fit each average power spectrum, from which the centroid Doppler-shifted frequency is estimated.

In order to measure the three wind velocity components in the ABL, the WindCube (as the ZephIR) is arranged to scan the atmosphere conically from the ground. The laser beam is tilted at an angle ϕ from the zenith, thus, it is able to measure the radial velocity vector, $\boldsymbol{v_r}$, as a function of the wind velocity vector, $\boldsymbol{u}$. The wind speed components, i.e. u, v and w, can be derived by measuring at different azimuth angles, θ. This is illustrated in Fig. 2.4 where the WindCube measures the radial velocity at four points separated by 90°.

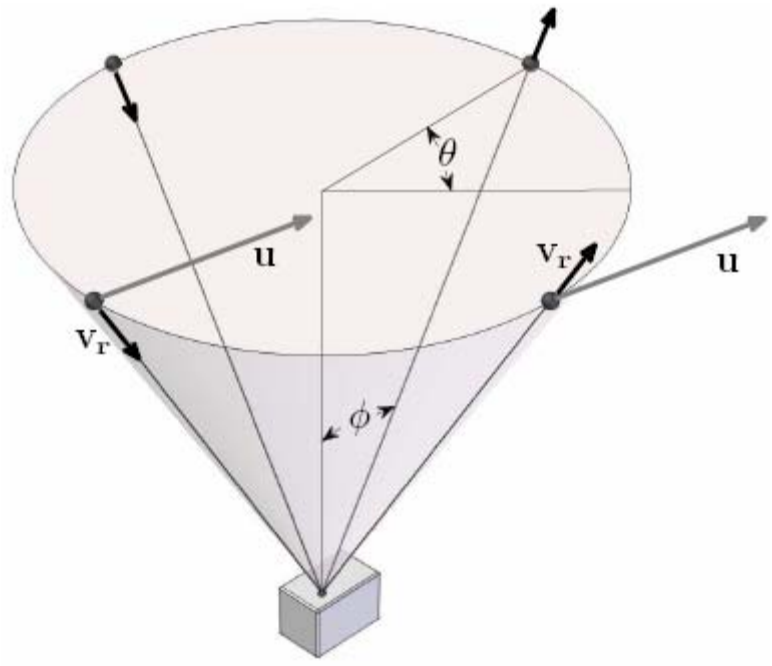

Figure 2.4 Scanning configuration of the WindCube lidar.

2.3 The winter campaign

During the winter campaign, a WindCube was installed at the tall meteorological mast and programmed to perform measurements at 10 different heights 60, 80, 100, 116, 130, 160, 200, 250 and 300 m. The main objective of the campaign was the investigation of the near-neutral wind profile and its departures from the traditional surface-layer theory.

2.3.1 Theory

Traditional theory states that the neutral surface-layer length scale $(l_{sl})_N$ grows proportionally with height z as:

$$(l_{sl})_N = \kappa z \tag{2.4}$$

where κ is the von Kármán constant (≈ 0.4). The wind profile can then be derived by integrating the wind shear $\partial U/\partial z$ (where U is the mean wind speed), because this is proportional to the ratio between the velocity scale (the surface friction velocity u_{*o}) and the length scale:

$$\frac{\partial U}{\partial z} = \frac{u_{*o}}{(l_{sl})_N} = \frac{u_{*o}}{\kappa z}. \tag{2.5}$$

The result of the integration of Eq. (2.5) with height is the well-known logarithmic wind profile:

$$U = \frac{u_{*o}}{\kappa} \ln\left(\frac{z}{z_o}\right) \tag{2.6}$$

where z_o is the surface roughness length. Beyond surface layer, the logarithmic wind profile is not valid, because we cannot longer assume that the length scale grows

infinitively with height and that the stress (the friction velocity) is constant. Because we can retrive observations at high heights with the lidars, we need to compare the observations with wind- and length-scale profiles, which limit the growth of the length scale above the surface layer. This was explain in detail in Peña *et al.* (2008) and here we show the main features. For the length scale, we used the following limiting length-scale models:

$$l = \frac{\kappa z}{1 + \left(\frac{\kappa z}{\eta}\right)^d}, \tag{2.7}$$

$$l = \eta \tanh\left(\frac{\kappa z}{\eta}\right), \tag{2.8}$$

$$l = \left(\frac{1}{\kappa z} + \frac{1}{\kappa l_{MBL}} + \frac{1}{\kappa(z_i - z)}\right) \tag{2.9}$$

where η is a limiting value for the length scale in the upper atmosphere, p is related with the gradient of the length scale (Blackadar 1962 used $d = 1$ and Lettau 1962 used $d = 5/4$), z_i is the boundary-layer height, and l_{MBL} is a middle boundary-layer length scale (Gryning *et al.* 2007). Hereafter we will call the model in Eq. (2.7) with $d = 1$ "Blackadar's model", Eq. (2.7) with $d = 5/4$ "Lettau's model", Eq. (2.8) "Panofsky's model", and Eq. (2.9) "Gryning's model".

A number of analytical wind profile models can be obtained by integration of the local wind shear, as shown before for the surface layer in Eq. (2.5), but using the ratio of the local friction velocity u_*, and the local length scale l. We used the model proposed by Panofsky (1973) for the decrease of wind stress with height:

$$u_* = u_{*o}\left(1 - \frac{z}{z_i}\right). \tag{2.10}$$

The result of the integration with height of the combination of the length-scale models, Eqs. (2.7)−(2.9), with the friction velocity model in Eq. (2.10), gives:

$$U = \frac{u_{*o}}{\kappa}\left[\ln\left(\frac{z}{z_o}\right) + \frac{1}{d}\left(\frac{\kappa z}{\eta}\right)^d - \left(\frac{1}{1+d}\right)\frac{z}{z_i}\left(\frac{\kappa z}{\eta}\right)^d - \frac{z}{z_i}\right] \tag{2.11}$$

$$U = \frac{u_{*o}}{\kappa}\left[\ln\left(\frac{\sinh(\kappa z/\eta)}{\sinh(\kappa z_o/\eta)}\right) - \frac{\kappa z}{2\eta}\frac{z}{z_i}\right] \tag{2.12}$$

$$U = \frac{u_{*o}}{\kappa}\left[\ln\left(\frac{z}{z_o}\right) + \frac{z}{l_{MBL}} - \frac{z}{z_i}\frac{z}{2l_{MBL}}\right], \tag{2.13}$$

which we will call Blackadar's, Lettau's, Panofsky's and Gryning's wind profile models in analogy to the length-scale model used for their derivation. The boundary-layer height is estimated with the Rossby-Montgomery formula:

$$z_i = C\frac{u_{*o}}{|f_c|}$$

where f_c is the Coriolis parameter and C is a proportionality constant (≈ 0.15).

2.3.2 Results for the Leipzig wind profile

The limiting value for the length scale, η, in the equations above, was estimated first by fitting the length-scale models, Eqs. (2.7)−(2.9), to the well-known Leipzig wind

profile, which Lettau (1950) re-analyzed resulting in a length-scale profile and a wind profile that have been used for the study of the neautral and barotropic atmosphere. The main results are shown in Fig. 2.5. In general, the limiting length-scale models and their derived wind profiles fit better the observations above the surface layer than the traditional theory.

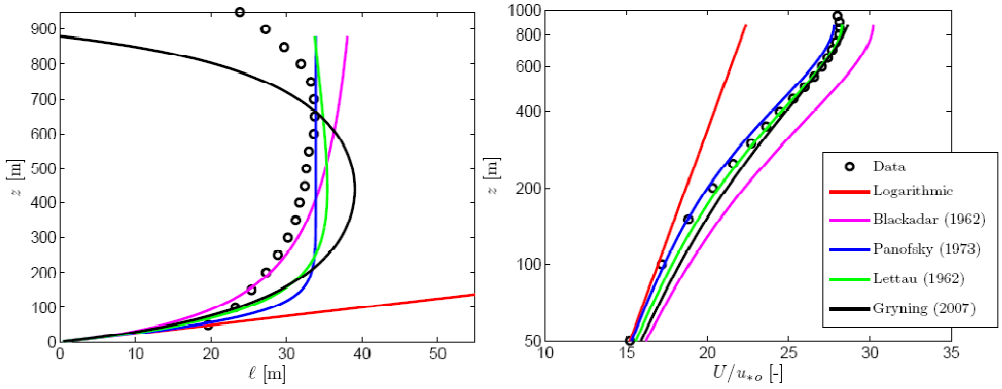

Figure 2.5 Length-scale (left panel) and wind speed (right panel) profiles for the Leipzig wind profile (Data).

2.3.2 Results for the Høvsøre wind profile

For the study of the length-scale and the wind profiles at Høvsøre, the data from the lidar and the instruments at the meteorological mast were stored as 10-min averages. Only wind speeds above 2 m s^{-1} were used and the wind sector is selected based on the observation at 10 m. Near-neutral conditions are selected based on the estimation of the Obukhov length, L, from the kinematic fluxes observed with a sonic at 10 m at the meteorological mast:

$$L = \frac{-u_{*o}^3 T_o}{\kappa g \overline{w'\Theta_v'}_o} \tag{2.14}$$

where T_o is the surface-layer mean temperature, g the gravitational acceleration, and $\overline{w'\Theta_v'}_o$ the surface-layer kinematic heat flux. The selection was performed on the range $|L| \geq 500$.

Fig. 2.5 shows a good agreement for the horizontal wind speed obsevations of the lidar when compared to the cup anemometer wind speeds at 116 m. Table 2.1 gives the main surface parameters found during the campaign in conjunction with the historical values from the cup anemometers, which have observed winds continously for more than three years under the same sector and stability conditions. The logarithmic wind profile was fitted to the campaign and historical datasets at the height 10 m to derive the roughness length.

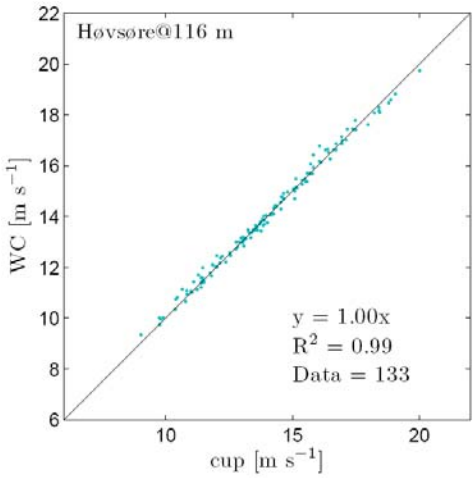

Figure 2.5 Comparison of horizontal mean wind speed between the WindCube (WC) lidar and the cup at 116 m at Høvsøre, Denmark.

Data	No. of observations	U_{10} [m s^{-1}]	u_{*o} [m s^{-1}]	$\overline{w'\Theta_v'}_o$ [m s^{-1} K]	z_o [m]
Campaign	133	9.88	0.61	0.0048	0.016
Historical	4614	7.57	0.47	0.0008	0.016

Table 2.1 Mean surface parameters observed at 10 m under near-neutral conditions.

The wind speed measurements observed with the cup anemometers were combined with the lidar observations at higher heights. In Fig. 2.6, the length-scale and mean wind speed profiles observed during the campaign and the historical data are compared with the models. The values for the limiting length scales were selected in correspondance to the results observed from the comparison of the models to the Leipzig wind profile data. As shown previously with the results for the Leipzig wind profile, the limiting length scale models fit better the observations than compared to the traditional theory. For the wind profile, the fit is also better than compared to the traditional theory, expect for Blackadar's model, which overestimates strongly the wind speed compared to all models.

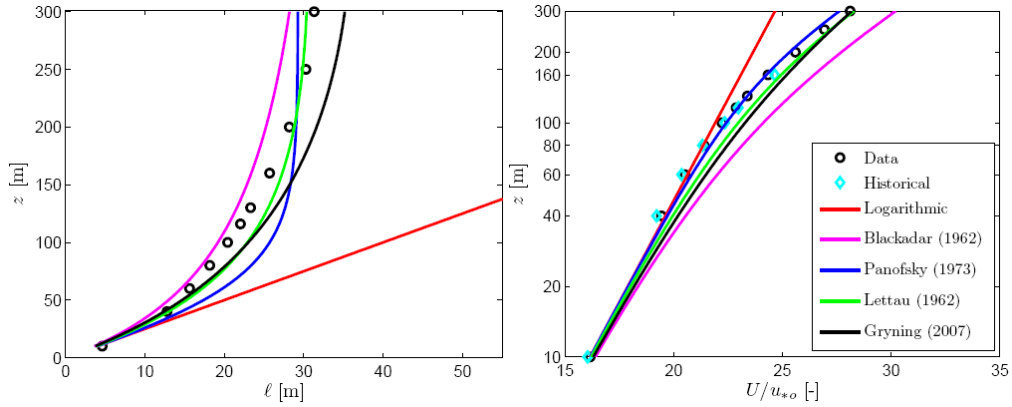

Figure 2.6 Length-scale (left panel) and mean wind speed (right panel) profiles at Høvsøre for the lidar campaign (Data). The historical mean wind profile is also shown in the right panel.

From the records of sonic anemometer observations performed for about one year at Høvsøre, up to 160 m, we were able to analyze the behavior of the length scale derived from a spectral analysis and compare it to the length scale of the wind profile

derived from the wind shear analysis, i.e. estimating the local length scale from the ratio of the friction velocity and wind shear, i.e. $l = u_*/(\partial U/\partial z)$. 617 10-min time series were used for the study with the sonic measurements.

Two spectral models were fitted to the average normalized spectra (averaged on the normalized frequency, $n = fz/U$, where f is the frequency in Hz) of the u and w wind velocity components and uw covariance, $fS_{u,w}(f)/u_*^2$ and $fC_{uw}(f)/u_*^2$:

1. The Mann (1994) spectral model, which adjusts a length scale L_M, a measure of the energy dissipation and a parameter related to the degree of anisotropy to the velocity tensor.
2. The Kaimal *et al.* (1972) spectral model, which is represented by:

$$\frac{fS_u(f)}{u_*^2} = \frac{102n}{(1+33n)^{5/3}}, \tag{2.15}$$

$$\frac{fS_w(f)}{u_*^2} = \frac{2.1n}{1+5.3^{5/3}}, \tag{2.16}$$

$$\frac{-fC_{uw}(f)}{u_*^2} = \frac{12n}{(1+9.6n)^{7/3}}. \tag{2.17}$$

The wavelength of the spectral peak, λ_m, is estimated from the Kaimal model fit. The results of the fitted spectra are shown in Fig. 2.7. The Mann model fits well the u and w spectra and overestimates the uw co-spectra at all heights, whereas the Kaimal model fits well all spectra at low heights, but overestimates the u spectra at higher levels and the uw co-spectra at 160 m.

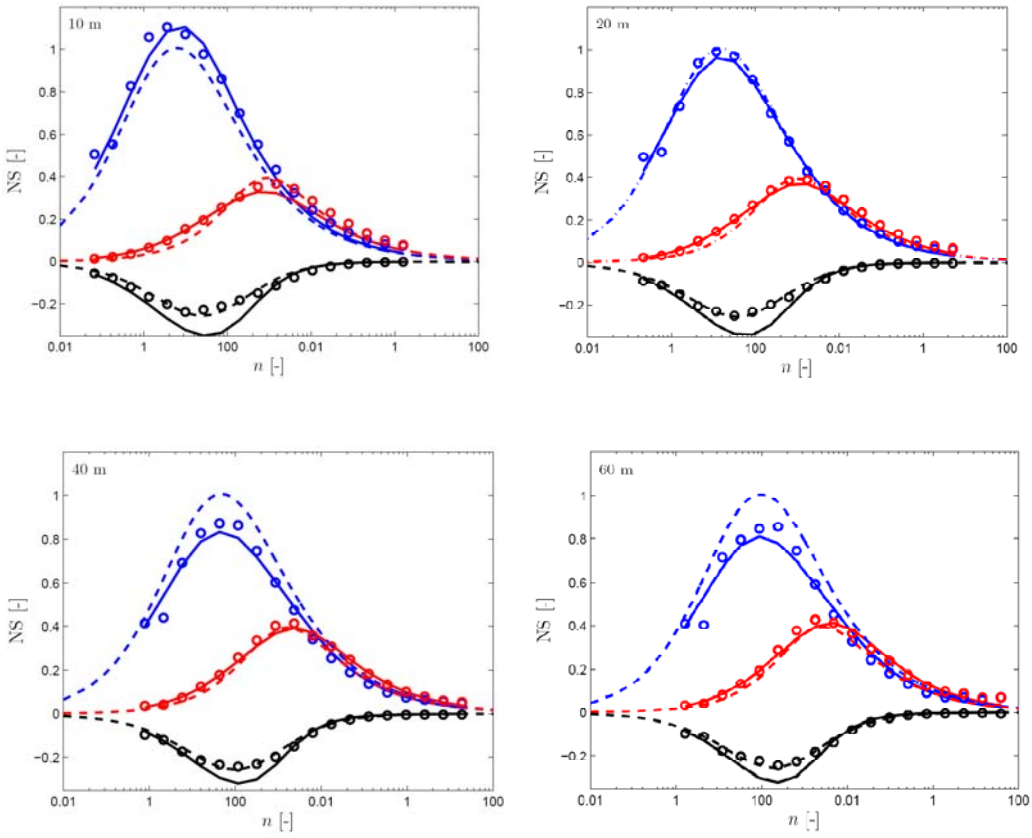

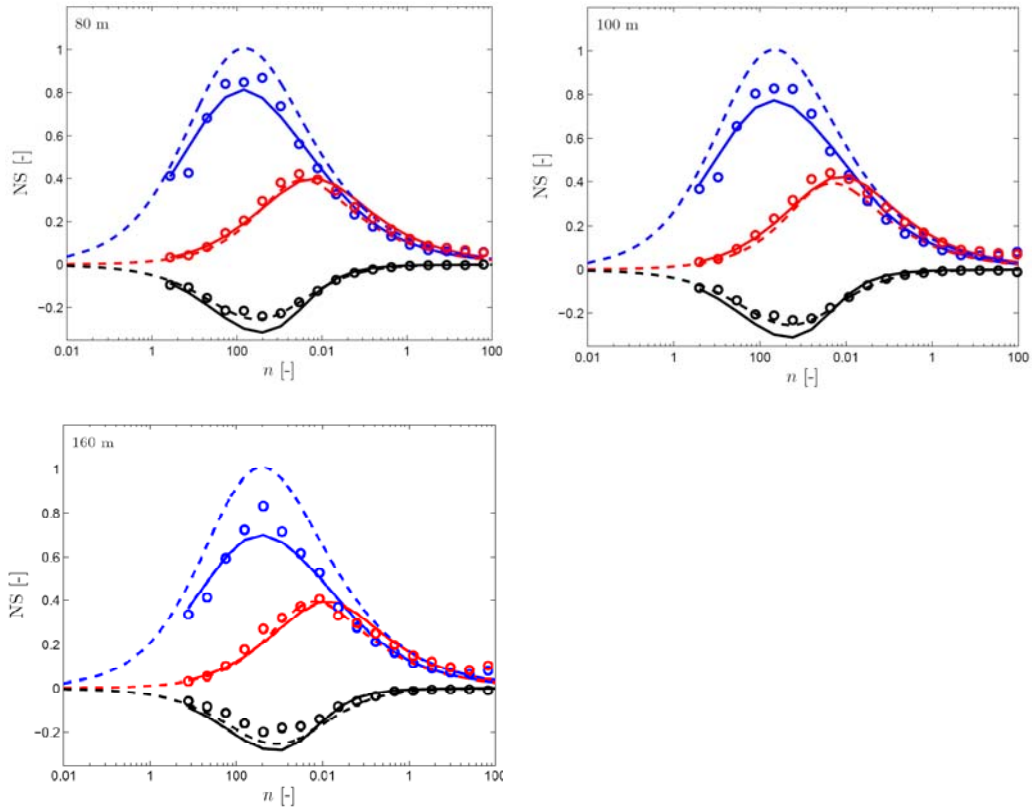

Figure 2.7 Normalized spectra and co-spectra (NS) of u (blue), w (red) and uw (black) for normalized frequencies from the analysis of sonic observations at different heights at Høvsøre. The observations are shown in circles, the fit with the Kaimal model in dashed lines, and the Mann model fit in solid lines.

Length-scale profiles can be derived from the wind speed observations by using either the friction velocity model, Eq. (2.10), (hereafter Data-m), or the local friction velocity measured by each sonic (Data-l). These are shown in Fig. 2.8 and compared to the length-scale models and the estimations of the spectral length scale using Mann's model. A parameter β is used to relate the spectral-length scale with the length-scale of the profile. We used a value of 0.438 for β based on the observations performed by Mann (1994) at a flat-bottomed fjord on the Danish island of Zealand. The length scale derived from the wind shear (Data-m) and the one estimated from Mann (1994) shows good agreement at all heights, as illustrated in Fig. 2.8. The limiting length scale models also fit well the measurements at all heights.

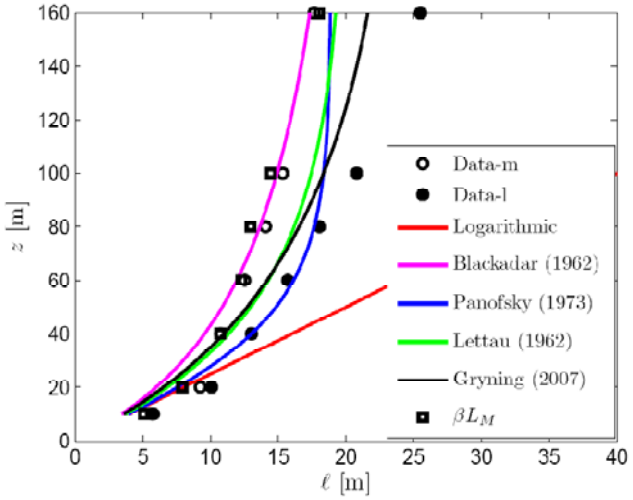

Figure 2.8 Length-scale profiles from the sonic anemometers at Høvsøre compared to the length scale derived from the Mann (1994) spectral model and the near-neutral limiting length-scale models.

From Mann (1994), the relation between L_M and the spectral peaks, which might be estimated by using the Kaimal model, can be derived. Thus, the w-spectrum and the uw-co-spectrum wavelength peaks can be also related to the length scale of the profile as:

$$l = \frac{\beta(\lambda_m)_w}{2\pi 0.5}$$
$$l = \frac{\beta(\lambda_m)_{uw}}{2\pi 2.3}.$$

Fig. 2.9 also illustrates an excellent agreement between the spectral peaks and the length scale derived from the wind shear and the limiting length-scale models.

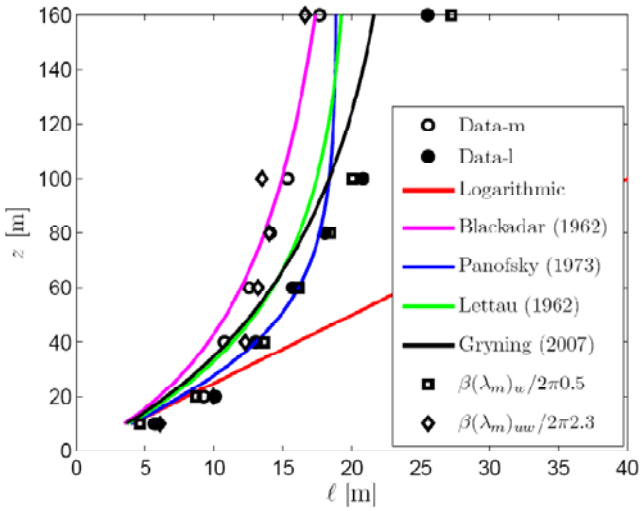

Figure 2.9 Length-scale profiles from the sonic anemometers at Høvsøre compared to the length scale derived from the spectral peaks using the Kaimal spectral model and the near-neutral limiting length scale models.

The results of this campaign are shown in great detail in Peña *et al.* (2008)

2.4 The summer campaign

Another WindCube wind lidar was installed at the meteorological mast during the summer campaign. It also performed measurements at 60, 80, 100, 116, 130, 160, 200, 250 and 300 m. The main objective of the campaign was the investigation of the diabatic wind profile, i.e. the varitation of the wind profile due to different stability conditions, and its departures from the traditional surface-layer theory.

2.4.1 Theory

In order to take into account the stability of the atmosphere in the models, we make use of Monin-Obukhov similarity theory (MOST), which extends the wind shear using an universal function of the dimensionless stability, z/L, in the surface layer:

$$\frac{\partial U}{\partial z} = \frac{u_{*o}}{\kappa z}\phi_m \tag{2.18}$$

where ϕ_m is the so-called dimensionless wind shear, which has been computed from different meteorological campaigns (Businger *et al.* 1971, Högström 1988), from which the following flux-profile relationships have been found, for unstable and stable conditions, respectively:

$$\phi_m = \left(1 - a\frac{z}{L}\right)^p \tag{2.19}$$

$$\phi_m = 1 + b\frac{z}{L}. \tag{2.20}$$

When the wind shear in Eq. (2.18) is integrated using Eqs. (2.19) and (2.20), the traditional surface-layer wind profile is obtained:

$$U = \frac{u_{*o}}{\kappa}\left[\ln\left(\frac{z}{z_o}\right) - \psi_m\right] \tag{2.21}$$

Where ψ_m is the extension used in traditional surface-layer theory to the logarithmic wind profile for diabatic conditions and its form depends on the ϕ_m function.

The extension for diabatic conditions on the limiting length-scale models can be easily performed, because Eqs. (2.7) and (2.9) can be studied as the inverse summation of different length scales in the atmosphere. Gryning *et al.* (2007) showed how to perform that extension using their length-scale model. The addition of the ϕ_m function into Eq. (2.7) is now combined with the friction velocity model in Eq. (2.10) resulting in the local diabatic wind shear:

$$\frac{\partial U}{\partial z} = u_{*o}\left(1 - \frac{z}{z_i}\right)\left(\frac{1}{\kappa z}\phi_m + \frac{(\kappa z)^{d-1}}{\eta^d}\right). \tag{2.22}$$

Then, integrating Eq. (2.22) with height using the forms in Eqs. (2.19) and (2.20), the diabatic wind profiles are, for neutral, unstable and stable conditions, respectively:

$$U = \frac{u_{*o}}{\kappa}\left[\ln\left(\frac{z}{z_o}\right) + \frac{1}{d}\left(\frac{\kappa z}{\eta}\right)^d - \left(\frac{1}{1+d}\right)\frac{z}{z_i}\left(\frac{\kappa z}{\eta}\right)^d - \frac{z}{z_i}\right] \tag{2.23}$$

(2.24)

$$U = \frac{u_{*o}}{\kappa}\left[\ln\left(\frac{z}{z_o}\right) - \psi_m + \frac{1}{d}\left(\frac{\kappa z}{\eta}\right)^d - \left(\frac{1}{1+d}\right)\frac{z}{z_i}\left(\frac{\kappa z}{\eta}\right)^d - \frac{z}{z_i}\right]$$
$$U = \frac{u_{*o}}{\kappa}\left[\ln\left(\frac{z}{z_o}\right) + b\frac{z}{L}\left(1 - \frac{z}{2z_i}\right) + \frac{1}{d}\left(\frac{\kappa z}{\eta}\right)^d - \left(\frac{1}{1+d}\right)\frac{z}{z_i}\left(\frac{\kappa z}{\eta}\right)^d - \frac{z}{z_i}\right] \quad (2.25)$$

2.4.2 Results

Data from the lidar and the instruments at the meteorological mast were stored as 10-min averages. Only wind speeds above 2 m s^{-1} were used and the wind sector is selected based on the observation at 10 m. The stability conditions are selected based on the Obukhov length estimated from the kinematic fluxes observed with a sonic at 10 m at the meteorological mast. The intervals of Obukhov lengths shown in Table 2.2 are used to classify the 10-min measurements into different stability conditions.

Obukhov length interval [m]	Atmospheric stability class
$10 \leq L \leq 50$	Very stable (vs)
$50 \leq L \leq 200$	Stable (s)
$200 \leq L \leq 500$	Near stable (ns)
$\|L\| \geq 500$	Neutral
$-500 \leq L \leq -200$	Near unstable (nu)
$-200 \leq L \leq -100$	Unstable (u)
$-100 \leq L \leq -50$	Very unstable (vu)

Table 2.2 Atmospheric stability classes according to intervals of Obukhov lengths.

As in the winter campaign, the observations of horizontal wind speed of the lidar compared well to the cup anemometer at the meteorological mast. Figure 2.10 shows the worst agreement found for the lidar/cup comparison, which corresponds to the cup at 160 m on the light tower, north of the meteorological mast.

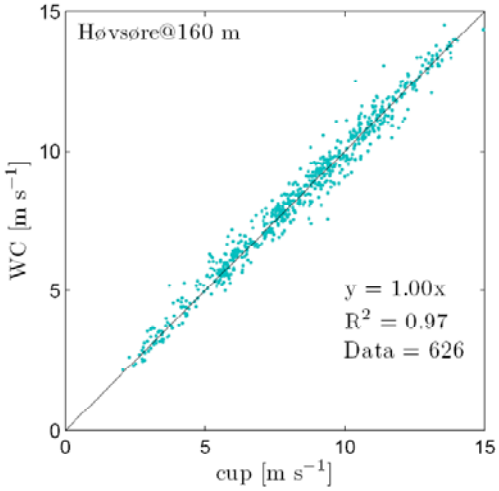

Figure 2.10 Comparison of horizontal mean wind speed between the WindCube (WC) lidar and the cup at 160 m at Høvsøre, Denmark.

For each stability class, an average was performed for the 10-min combined lidar/cup anemometer wind profiles and for the 10-min parameters required for the models. The roughness length was estimated from Eq. (2.21) using the measurements at 10 m only. The mean parameters for the campaign are given in Table 2.3.

Stability class	No. of profiles	u_{*o} [m s^{-1}]	z_o [m]	z_i [m]	L [m]
vs	75	0.13	0.006	105	27
s	143	0.25	0.027	251	115
ns	125	0.35	0.034	434	321
n	104	0.40	0.045	498	2771
nu	61	0.39	0.047	467	-334
u	63	0.41	0.046	571	-143
vu	45	0.38	0.044	563	-74

Table 2.3 Estimated mean parameters for the wind profiles in each stability class.

For the test of the wind profile models, z_i is estimated with the Rossby-Montgomery formula for neutral and all stable conditions. For unstable conditions, it is derived from ceilometer observations of the aerosol backscatter profile. The estimation of z_i from the average 10-min aerosol profile is illustrated in Fig. 2.11.

Fig. 2.12 illustrates the comparison of the observations with the traditional surface-layer theory, Eq. (2.21). The predicted wind profiles fit the observations in the first meters only. Beyond the surface layer, there is a clear under- and over-estimation of the wind speed at around 100 m for unstable conditions, 60 m for neutral conditions and 40 m for stable conditions.

Fig. 2.13 illustrates the comparison of the observations with the Gryning's wind profile models for the best estimate of l_{MBL} from the measurements. It is clear that the predictions with this model are much closer to the measurements than those shown in Fig. 2.12. For the first meters above the ground in unstable conditions, the fit is not accurate, because the model tries to correct for the kink of the profile at around 130 m.

Figs. 2.14 and 2.15 illustrate the comparison between the observations and the extended models of Blackadar (1962) and Lettau (1962) for the best estimate of η from the measurements. The predictions fit the observations as well as shown for the wind profiles of Gryning *et al.* (2007). A slightly better prediction is observed by using $d = 5/4$ compared to Gryning's and Blackadar's models within the first tens of meters for the near-neutral wind profiles. Similar results were found for the winter campaign (Peña *et al*. 2008).

The results of this campaign are shown in great detail in Peña *et al.* (2009b)

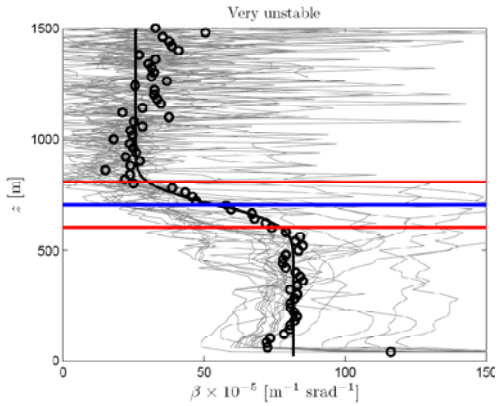
Very unstable
z [m]
β × 10⁻⁵ [m⁻¹ srad⁻¹]

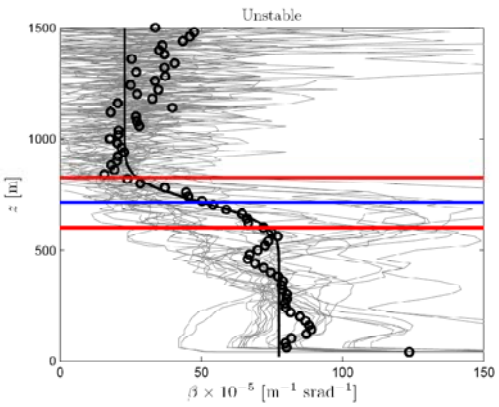
Unstable
z [m]
β × 10⁻⁵ [m⁻¹ srad⁻¹]

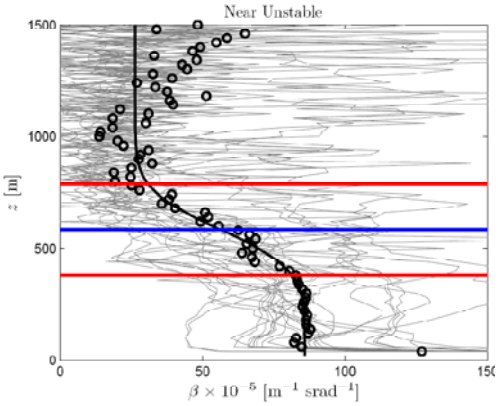
Near Unstable
z [m]
β × 10⁻⁵ [m⁻¹ srad⁻¹]

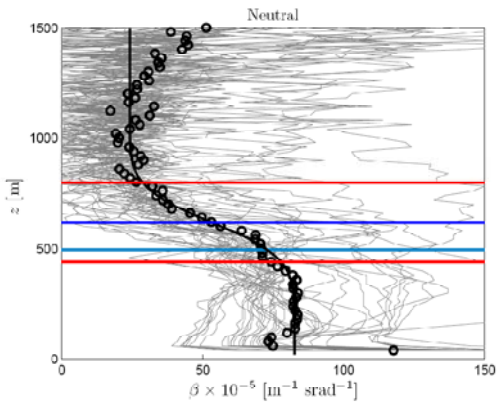
Neutral
z [m]
β × 10⁻⁵ [m⁻¹ srad⁻¹]

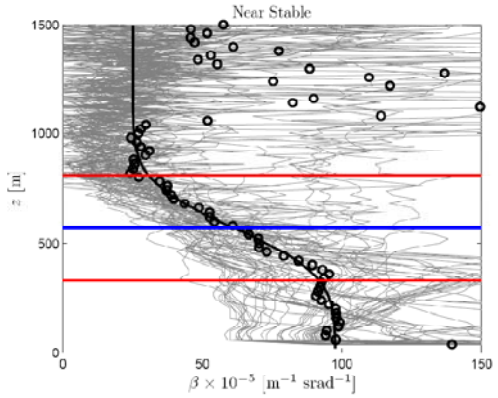
Near Stable
z [m]
β × 10⁻⁵ [m⁻¹ srad⁻¹]

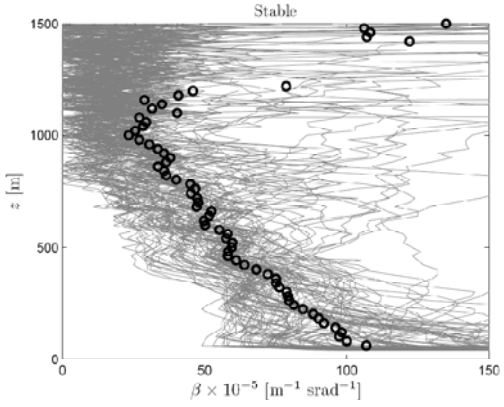
Stable
z [m]
β × 10⁻⁵ [m⁻¹ srad⁻¹]

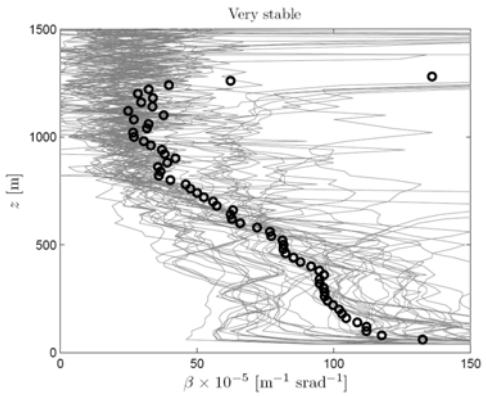

Figure 2.11 Ceilometer observations of aerosol backscatter β for different stability conditions. The 10-min observations are shown in light gray and the mean in circles. The boundary-layer height (blue line) is estimated by fitting an error function (black line) to the mean of the observations. The red lines correspond to the entrainment zone from the aerosols.

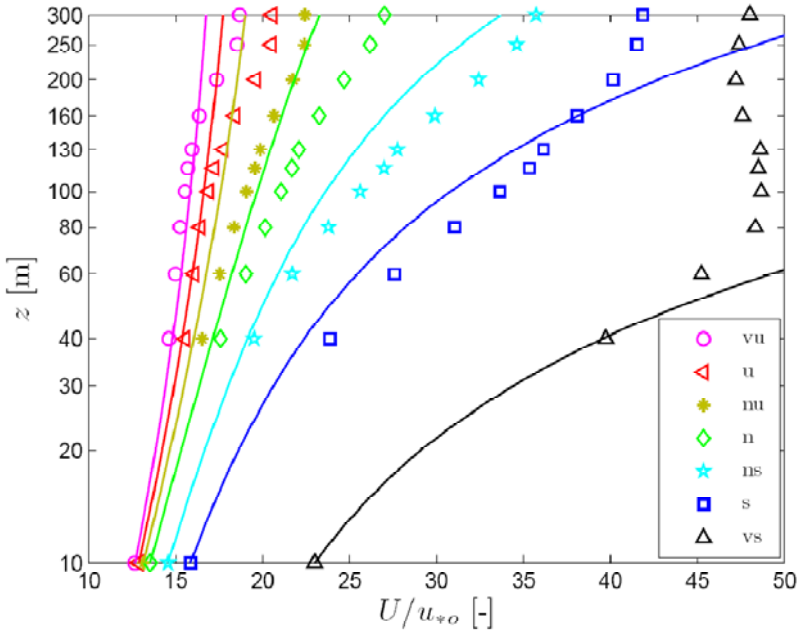

Figure 2.12 Comparison of combined cup/lidar observations (markers) and the wind speed profile from traditional surface-layer theory (solid lines) for each stability class.

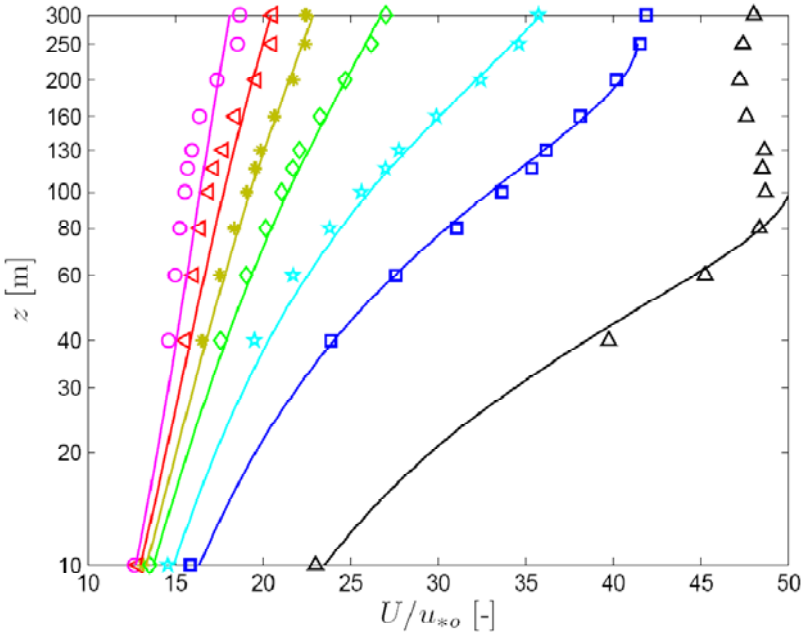

Figure 2.13 The same as Fig.2.12 but using the wind profiles models by Gryning et al. (2007).

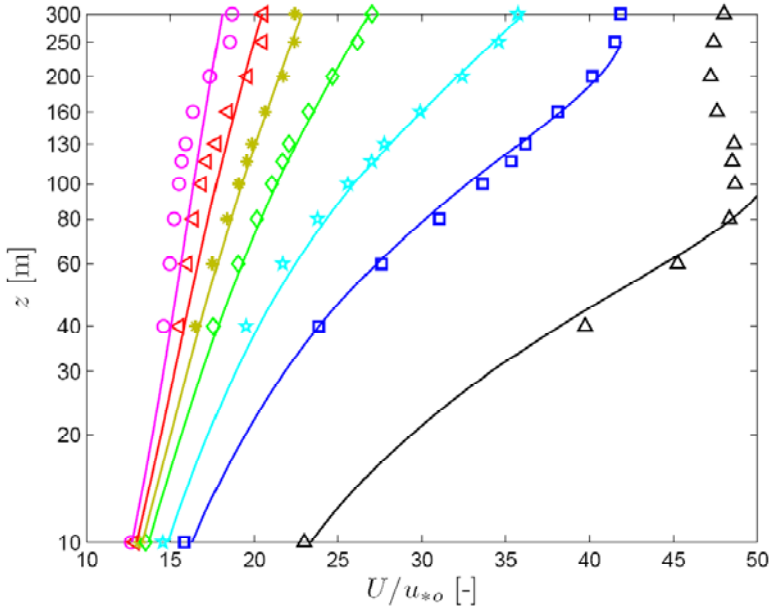

Figure 2.14 The same as Fig.2.12 but using the extended Blackadar's wind profile models, Eqs. (2.23)−(2.25), with $d = 1$.

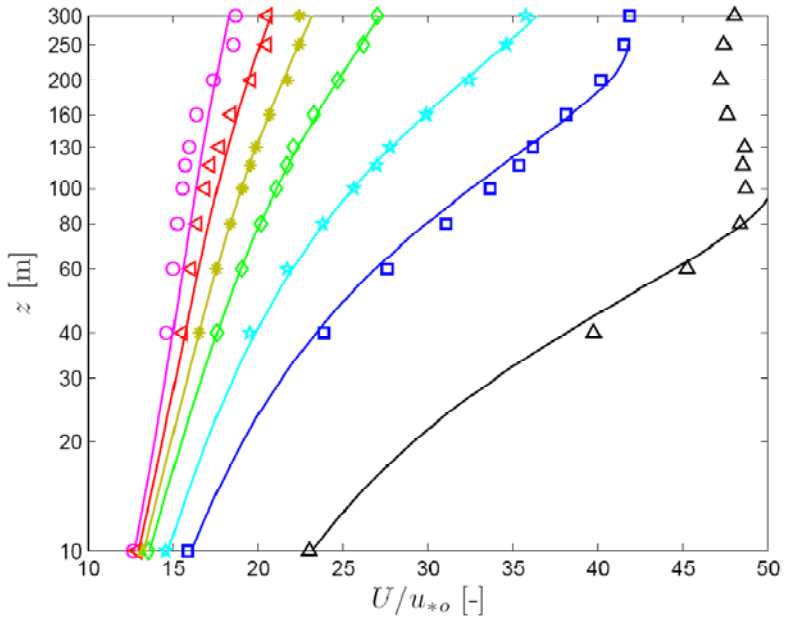

Figure 2.15 The same as Fig.2.12 but using the extended Lettau's wind profile models, Eqs. (2.23)−(2.25), with $d = 5/4$.

2.5 Summary on the Høvsøre experiment

The wind profile in and beyond the surface layer has been measured over flat and homogenous terrain at the National Test Station for Wind Turbines at Høvsøre, Denmark, by combining traditional wind speed measurements from cup anemometers with lidar observations. Such combination was possible, due to the high correlation and agreement between the traditional instruments and the lidar sensing technique found at all the possible lidar/cup overlapping heights.

The wind speed measurements showed a good agreement compared to the traditional surface-layer wind profile in the layer of the atmosphere where the surface layer is extended and for a wide range of atmospheric stability conditions. The comparison was accomplished by averaging the 10-min wind profile measurements for similar stability conditions, based on intervals of Obukhov lengths observed from the turbulent fluxes from sonic anemometer measurements close to the ground and by scaling the mean horizontal wind speed with the surface-layer friction velocity.

Wind speed measurements performed up to 300 m in near-neutral stability conditions showed a wind speed over-speeding when compared to the logarithmic wind profile, as observed from the reanalysis of the Leipzig wind profile up to 950 m. The length scale of the wind profile, derived from wind speed measurements, was compared to several length-scale models showing a notably better agreement than compared to the indefinitely increasing surface-layer length scale. Wind profile models, derived from those length-scale models, which also take the boundary-layer height into account, compared better to the wind speed measurements from Leipzig and Høvsøre than the logarithmic wind profile.

The neutral length scale derived from a spectral analysis of turbulence measurements at Høvsøre up to 160 m, further beyond the surface layer, was proportional to the length scale derived from the wind speed profiles, in agreement with the findings within the surface layer of Mann (1994) at a flat bottomed fjord on Zealand, Denmark.

Two length-scale models were extended to account for a wide range of stability conditions, as MOST corrects the surface-layer length scale, and used to derive wind profile models for flow over flat land and homogeneous terrain where the boundary-layer height was included as a scaling parameter for the whole range of stability conditions, as shown in the models of Gryning et al. (2007). The derived wind profile models and those of Gryning et al. (2007) were particularly better when compared to the surface-layer wind profile, by analyzing wind speed measurements up to 300 m at Høvsøre for near-neutral and stable conditions. For unstable conditions, an over-speeding was not predicted by the traditional wind profile, but followed by the other models.

Ceilometer measurements also averaged within intervals of Obukhov lengths, showed a characteristic aerosol backscatter profile, which was useful to estimate the boundary-layer height in near-neutral and unstable conditions.

3 Turbulence

A note on the stream-wise measured Variances and Turbulence intensities measured by Conical Scanning VAD LIDARs (e.g. ZephIR)

Torben Mikkelsen
May 27. 2009

Note prepared for "12 MW – Final Report"

When a wind lidar is operating conical scanning Velocity Azimuth Display (VAD) mode, it measures several (e.g. 50) radial wind components equally spaced (e.g. every 7.2 degrees) per revolution (360 degree cone scan). A cone is scanned often (e.g. once per second).

From each VAD scans (one per second) the wind speed and direction can be extracted, e.g. via period –average harmonic analysis (Eberhard et al. 1989). These estimates can then be averaged together, e.g. by averaging 600 wind speed estimates over a 10-min period, to form the lidar measured 10- min mean wind speed.

However, also the stream-wise variance and hence the stream- wise turbulence intensity can also be derived. This will be done next:

Assume homogeneous stationary flow $\mathbf{V}(x,y,z)=(V_x, V_y, V_z)$ where V_x, V_y and V_z are the components of the flow velocity vector $\mathbf{V}$ being a random function of the spatial coordinates $\mathbf{r}=\{x,y,z\}=\{z\cos\varphi\cos\theta,\ z\cos\varphi\sin\theta,\ z\sin\varphi\}$, where θ is the rotating azimuth angle and φ is the elevation angle determined by the rotating prism.

Definitions:

A wind lidar scanning in the so-called "Velocity Azimuth Display" (VAD) mode, i.e. conically scanning, measures the radial component of the velocity vector:

$$V_r = V_x\cos\varphi\cos\theta + V_y\cos\varphi\sin\theta + V_z\sin\varphi \qquad (0.1)$$

Using this scanning technique the three wind components $\{V_x, V_y, V_z\}$ can be obtained from harmonic analysis of the radial wind speed V_r's dependence on the azimuth angle θ.

Assuming e.g. that a full 2π scan is performed once every second, the corresponding one-second averaged estimate of the wind vector is:

$$\mathbf{V} = \frac{1}{2\pi}\int_0^{2\pi} V_r(\theta)\ \mathbf{A}(\theta)\, d\theta, \qquad \text{where}$$

$$\mathbf{A} = \{2\cos\theta/\cos\varphi,\ 2\sin\theta/\cos\varphi, 1/\sin\varphi\}.$$

For example, for the 1-s averaged streamwise wind component, we have

$$V_x = \frac{1}{\cos\varphi}\frac{1}{\pi}\int_0^{2\pi} V_r(\theta)\cos(\theta)d\theta. \qquad (0.2)$$

Assuming Tailors' frozen turbulence approximation applies over the cone volume and that a full 2π scanning is performed once per second over, say, a 10- min period, we have, for instance for the lidar-measured stream wise wind component, for the i^{th} second:

$$< V_x >_i = \frac{1}{\cos\varphi}\frac{1}{\pi}\int_0^{2\pi} V_r(\theta)\cos(\theta)d\theta \quad (0.3)$$

We can easily calculate the variance in a time series of this quantity, if we assume that any two measurements are independent of one another, in practise this will be true if the time series is "long enough". Alternatively, we can proceed formally by introducing the co-variance function:

(0.4)

$$< V_x >_{t_i} = \frac{1}{\cos\varphi}\frac{1}{\pi}\int_0^{2\pi} V_r(t_i,\theta)\cos(\theta)d\theta$$

$$< V_x >_{t_j} = \frac{1}{\cos\varphi}\frac{1}{\pi}\int_0^{2\pi} V_r(t_j,\theta)\cos(\theta)d\theta$$

and hence

$$R_x(t_i - t_j) = < V_{x,t_i} V_{x,t_j} >_{10-\min} = < \frac{1}{\cos\varphi}\frac{1}{\pi}\int_0^{2\pi} V_r(t_i,\theta')\cos(\theta')d\theta' \ \ \frac{1}{\cos\varphi}\frac{1}{\pi}\int_0^{2\pi} V_r(t_j,\theta'')\cos(\theta'')d\theta'' >_{10-\min}$$

where $R_x(t_i - t_j)$ is the Co-variance function for the 1-s time-averaged stream wise velocity fluctuations as measured by the conical scanning VAD lidar.

For instance, the stream wise VAD scanned variance can now be evaluated at zero time lag as:

(0.5)

$$R_x(0) = \langle V_{x,t_i} V_{x,t_i} \rangle_{10-\min} = \left(\frac{1}{\cos\varphi}\frac{1}{\pi}\right)^2 \int_0^{2\pi}\int_0^{2\pi} \langle V_r(t_i,\theta') V_r(t_i,\theta'') \rangle_{10-\min} \cos(\theta')\cos(\theta') d\theta' d\theta''$$

$$= \left(\frac{1}{\cos\varphi}\frac{1}{\pi}\right)^2 \cdot \pi \cdot \int_0^{2\pi} \langle V_r^2(\theta) \rangle_{10-\min} \cos^2(\theta)\, d\theta$$

$$= \left(\frac{1}{\cos\varphi}\right)^2 \cdot \frac{1}{\pi} \cdot \int_0^{2\pi} \langle V_r^2(\theta) \rangle_{10-\min} \cos^2(\theta)\, d\theta$$

The stream-wise VAD measured variance is seen to be determined by a "cosine square in space" weighting of the azimuth-scanned radial wind speed variance $\langle V_r^2(\theta) \rangle$.

Similar expressions can analogously be derived for the lateral and vertical VAD scanning derived variances.

The radial wind speed variance $\langle V_r^2(\theta) \rangle$:

Align a VAD scanning lidar so that the mean wind $\langle u \rangle$ is along the x direction and introduce Reynolds decomposition $V_x = \langle u \rangle + u'$, $V_y = v'$ and $V_z = w'$, assuming alignment so that $\langle v \rangle = 0$, $\langle w \rangle = 0$. The instantaneous measured radial wind speed, $V_r = \langle v_r \rangle + v_r'$, then becomes:

$$V_r(\theta) = \cos\varphi\cos\theta\ (\langle u \rangle + u') + \cos\varphi\sin\theta\ v' + \sin\varphi\ w';$$

$$\langle V_r \rangle_{2\pi}(\theta) = \cos\varphi\cos\theta \langle u \rangle$$

(0.6)

where φ is the lidar beams constant elevation angle and θ the scanning azimuth angle, which typically scan over 2π radians per second (cf. a ZephIR with $\varphi = 60^\circ$).

By squaring, averaging, and subtracting the (10-min) mean we obtain the measured radial wind speed variance $\langle v_r'^2(\theta) \rangle_{10-\min}$. As u' is positive along the x-axis, $\theta = 180$ denotes the upwind direction.

(0.7)

$$\langle v_r'^2(\theta) \rangle_{10-\min} = \left\langle \left(\cos\varphi\cos\theta u' + \cos\varphi\sin\theta v' + \sin\varphi w'\right)^2 \right\rangle$$

$$= \left\langle \begin{array}{l} \cos^2\varphi\cos^2\theta\, u'^2 + \cos^2\varphi\sin^2\theta\, v'^2 + \sin^2\varphi\, w'^2 + \\ \qquad 2\left(\cos^2\varphi\cos\theta\sin\theta u'v' + \sin\varphi\cos\varphi\cos\theta\ u'w' + \sin\varphi\cos\varphi\sin\theta v'w'\right) \end{array} \right\rangle$$

Assume the turbulence is homogeneous, so that the crosswind shear-stress terms may be neglected, i.e. $< u'v' > = < v'w' > \approx 0$. Then a simpler expression for the VAD scanning lidar's radial variance, as function of azimuth angle θ becomes:

(0.8)

$$\left\langle v_r'^2(\theta)\right\rangle_{10-\min} = \cos^2\varphi\cos^2\theta\left\langle u'^2\right\rangle + \cos^2\varphi\sin^2\theta\left\langle v'^2\right\rangle + \sin^2\varphi\left\langle w'^2\right\rangle + 2\sin\varphi\cos\varphi\cos\theta\left\langle u'w'\right\rangle$$

Next we assume standard relations between the variances and the friction velocity u_* in the surface layer, where by definition $-\left\langle u'w'\right\rangle \equiv u_*^2$. In homogeneous stationary surface layer turbulence the ratios between the three velocity components are, in according with standard Kaimal spectra:

$$\begin{aligned}
\frac{\sigma_u^2}{u_*^2} &= \int_0^\infty \frac{102}{(1+33n)^{5/3}}dn \approx 2.15^2, \\
\frac{\sigma_v^2}{u_*^2} &= \int_0^\infty \frac{17}{(1+9.5n)^{5/3}}dn \approx 1.64^2, \qquad (0.9)\\
\frac{\sigma_w^2}{u_*^2} &= \int_0^\infty \frac{2.1}{(1+5.3n^{5/3})}dn \approx 1.24^2.
\end{aligned}$$

Notably, the stream wise turbulence level (standard deviation) in Kaimal's spectral model is related to the friction velocity

$$\sigma_u \approx 2.15\, u_* \qquad (0.10)$$

The stream-wise VAD measured variance

Combining Eqs. (0.5) and Eqs.(0.8) now leads to the following expression for the VAD scanning lidar's stream wise fluctuating velocity variance,

(0.11)

$$< v_x v_x >_{VAD} = \left(\frac{1}{\cos\varphi}\right)^2 \cdot \frac{1}{\pi} \cdot \int_0^{2\pi} < v_r'^2(\theta) >_{10-\min} \cos^2(\theta)\, d\theta$$

$$\left\langle v_r'^2(\theta)\right\rangle_{10-\min} = \cos^2\varphi\cos^2\theta\left\langle u'^2\right\rangle + \cos^2\varphi\sin^2\theta\left\langle v'^2\right\rangle + \sin^2\varphi\left\langle w'^2\right\rangle + 2\sin\varphi\cos\varphi\cos\theta\left\langle u'w'\right\rangle$$

where $< v_x v_x > = < V_x V_x > - < u >_{10-\min}^2$ and $< v_r'^2(\theta) > = < V_r'^2(\theta) > - < v_r >_{10-\min}^2$, i.e. we have extracted the 10-min means.

Evaluation of Eqs. (0.11) require evaluation of the following integral (the last stress term integrates to zero being an odd function in θ):

(0.12)

$$< v_x v_x >_{VAD} = \left(\frac{1}{\cos\varphi}\right)^2 \cdot \frac{1}{\pi} \cdot \int_0^{2\pi} \left(\cos^2\varphi\cos^4\theta\left\langle u'^2\right\rangle + \cos^2\varphi\sin^2\theta\cos^2(\theta)\left\langle v'^2\right\rangle + \sin^2\varphi\cos^2(\theta)\left\langle w'^2\right\rangle\right)\, d\theta$$

With: $\int_0^{2\pi} \cos^4(\theta)\, d\theta = \pi$; $\int_0^{2\pi} \cos^2\theta \sin^2\theta\, d\theta = \frac{\pi}{4}$; $\int_0^{2\pi} \cos^2(\theta)\, d\theta = \pi$, we finally get:

(0.13)

$$< v_x v_x >_{VAD} = \left(\frac{1}{\cos\varphi}\right)^2 \cdot \frac{1}{\pi} \cdot \left(\pi \cos^2\varphi \langle u'^2 \rangle + \frac{\pi}{4}\cos^2\varphi \langle v'^2 \rangle + \pi \sin^2\varphi \langle w'^2 \rangle\right)$$

$$= \langle u'^2 \rangle + \frac{1}{4}\langle v'^2 \rangle + \tan\varphi \langle w'^2 \rangle$$

The VAD scanning lidar is seen to measure the correct stream wise variance, in addition to 25% of the lateral variance, and a contribution from the vertical component with a coefficient determined by Tangent to the elevation angle.

Example 1: For a standard ZephIR, with a 30 degree wedge, $\cos\varphi = ½;\ \sin\varphi = \frac{\sqrt{3}}{2};$ and $\tan\varphi = \sqrt{3}$, we obtain

$$< v_x v_x >_{ZephIR} = \langle u'^2 \rangle + \frac{1}{4}\langle v'^2 \rangle + \sqrt{3}\langle w'^2 \rangle \qquad (0.14)$$

Surface layer Kaimal turbulence:

If we adopt Kaimal Spectrum model for the three components:

$$< v_x v_x >_{ZephIR\,30^\circ} = 2.15^2 u_*^2 + \frac{1}{4} 1.64^2 u_*^2 + \sqrt{3} \cdot 1.24^2 u_*^2 \approx 2.82^2 u_*^2$$

we can estimate that the stream wise variance measured by a ZephIR equipped with a 30 degree wedge, relative to the stream wise variance of the turbulence, to be of the order of:

$$\frac{< v_x v_x >_{ZephIR30^\circ}}{\sigma_u^2} = \frac{2.82^2}{2.15^2} \sim 1.31^2$$

If we neglect filtering effects due to the finite sampling volume of the VAD scanning lidar, and assuming fully coherent turbulence over the entire VAD cone periphery, the anticipated turbulence intensity measured by a ZephIR lidar, relative to a cup anemometer, is here estimated to be 1.31 or + 31%.

Example 2: For a ZephIR, equipped with a 15 degree wedge, we have $\cos\varphi = 0.26;\ \sin\varphi = 0.97;$ and $\tan\varphi = 3.73$, and obtain

$$< v_x v_x >_{ZephIR\,15^\circ} = \langle u'^2 \rangle + \frac{1}{4}\langle v'^2 \rangle + \tan(75)\langle w'^2 \rangle \quad ,$$

(0.15)

$$\frac{< v_x v_x >_{ZephIR15^\circ}}{\sigma_u^2} = \frac{3.32^2}{2.15^2} \sim 1.54^2$$

that is, equipped with a 15 degree wedge, we should expect a slope in the lidar vs. cup intensity plot with a slope of as much as 1.54.

Conclusion

It has been shown that the stream wise turbulence intensity measured by a conical scanning lidar is "contaminated" by false contributions from both the crosswind and the vertical turbulence components.

The predicted correlation coefficient for the 10-min averaged intensity in a ZephIR vs. cup plot can theoretically range from 1.31 with a 30 degree wedge, and up to 1.54 with a 15 degree wedge.

However, smaller correlation coefficients are measured in real, which can be explained by this calculation methods neglect of :

1) coherence decorrelation over the cone volume, and
2) considering averaging over the lidar's finite sampling volume.

4 Databases

Alfredo Peña

Permission to access the two databases from Horns Rev and Høvsøre from the 12 MW project can be granted by Michael Courtney (mike@risoe.dtu.dk). Both databases are accessible from the server "veadbs-03.risoe.dk". You can also consult Alfredo Peña (aldi@risoe.dtu.dk) for more information concerning the structure of the database.

4.1 Horns Rev

The database for the Horns Rev project is called "hornsrev_platform". The following is a description of the most relevant tables. All values correspond to 10-min averages unless otherwise stated (in most cases the maximum, minimum and standard deviation values are also given). The data from the meteorological masts M2, M6 and M7 was kindly provided by Dong Energy, and in order to access them, permission should be granted.

Name	Channel	Description	Units
aq500_data		AQ500 sodar data	
	Name	Name of the time series	
	Height	Observational height	m
	Spd	Magnitude wind speed vector	m/s
	Dir	Direction	deg
	w	Wind speed vertical component	m/s
	u	Wind speed horizontal component	m/s
	v	Wind speed transversal component	m/s
	qual	Quality value from the unit	
m2_data		Meteorological mast 2	
	Name	Name of the time series	
	CUP62	Wind speed at 62 m AMSL	m/s
	CUP45SV	Wind speed at 45 m AMSL (south west boom)	m/s
	CUP45NO	Wind speed at 45 m AMSL (north east boom)	m/s
	CUP30SV	Wind speed at 30 m AMSL (south west boom)	m/s
	CUP30NO	Wind speed at 30 m AMSL (north east boom)	m/s
	CUP15SV	Wind speed at 15 m AMSL (south west boom)	m/s
	CUP15NO	Wind speed at 15 m AMSL (north east boom)	m/s
	DIR60SV	Direction at 60 m AMSL(south west boom)	deg
	DIR43SV	Direction at 43 m AMSL(south west boom)	deg
	DIR28NO	Direction at 28 m AMSL(north east boom)	deg
	TEMP55NO	Absolute temperature at 55 m AMSL (north east boom)	deg. C
	TEMP13NO	Absolute temperature at 13 m	deg. C

		AMSL (north east boom)	
	TEMPW	Absolute temperature at -4 m AMSL (under water)	deg. C
	HUM13NO	Relative humidity at 13 m AMSL (north east boom)	%
	BARP55NO	Absolute pressure at 55 m (north east boom)	hPa
	PYR13	Pyranometer	W/m^2
	RAIN	Rain gauge	mm
m6_data		Meteorological mast 6	
	Name	Name of the time series	
	CUP70	Wind speed at 70 m AMSL	m/s
	CUP60NW	Wind speed at 60 m AMS (north west boom)	m/s
	CUP50NW	Wind speed at 50 m AMSL (north west boom)	m/s
	CUP50SE	Wind speed at 50 m AMSL (south east boom)	m/s
	CUP40NW	Wind speed at 40 m AMSL (north west boom)	m/s
	CUP30NW	Wind speed at 30 m AMSL (north west boom)	m/s
	CUP30SE	Wind speed at 30 m AMSL (south east boom)	m/s
	CUP20NW	Wind speed at 20 m AMSL (north west boom)	m/s
	DIR68	Direction at 68 m AMSL	deg
	DIR28	Direction at 28 m AMSL	deg
	TEMP64	Absolute temperature at 64 m AMSL	deg. C
	TEMP16	Absolute temperature at 16 m AMSL	deg. C
	TEMPW	Absolute temperature at -4 m AMSL (under water)	deg. C
	BARP16	Absolute pressure at 16 m	hPa
m7_data		Meteorological mast 7 (The description is identical to mast 6)	
zephir_unit8_spectra		Raw frequency spectra	
	SpectraID	Identification number for spectra	
	freq	Doppler-shifted frequency	Hz
	sd	Spectral density (max=255)	
zephir_unit8_spectradef		Spectra analysis and definition	
	SpectraID	Identification number for spectra	
	Name	Name of the time series	
	Height	Measurement height	m
	Phase	Azimuthal position	rad
	Scaling	Spectra scaling factor	
	centroid	Doppler-shifted frequency at the centroid	Hz
zephir_unit8_calc10min		Statistics of the ZephIR wind lidar data	
	Name	Name of the time series	
	Height	Measurement height	m

	Points_in_fit	Number of points in the fit	
	Hor_vel	Magnitude of the horizontal wind speed	m/s
	Ver_vel	Magnitude of the vertical velocity	m/s
	Wind_Dir	Wind direction	deg

4.2 Høvsøre

The database for the Høvsøre project is called "hovsore". The following is a description of the most relevant tables used for the 12 MW project (the Høvsøre database is rather big and used for many different projects). All values correspond to 10-min averages and to the observations at the meteorological mast unless otherwise stated (in most cases the maximum, minimum and standard deviation values are also given):

Name	Channel	Description	Units
windcube_unit2_10min		Statistics of the WindCube wind lidar data (winter campaign)	
	Name	Name of the time series	
	Height	Measurement height	m
	Available	Amount of data available	%
	U	Horizontal wind speed	m/s
	Dir	Wind direction	Deg
	W	Vertical wind speed	m/s
	CNR	Signal to noise ratio	db
windcube_unit9_10min		Statistics of the WindCube wind lidar data (summer campaign). Description identical to windcube_unit2_10min	
calmeans		10-min statistics	
	Name	Name of the time series	
	Wsp_Metmast_116_5m	Cup wind speed at 116.5 m	m/s
	Wsp_Metmast_100m	Cup wind speed at 100 m	m/s
	Wsp_Metmast_80m	Cup wind speed at 80 m	m/s
	Wsp_Metmast_60m	Cup wind speed at 60 m	m/s
	Wsp_Metmast_40m	Cup wind speed at 40 m	m/s
	Wsp_Metmast_10m	Cup wind speed at 10 m	m/s
	Dir_metmast_100m	Direction at 100 m	Deg
	Dir_metmast_60m	Direction at 60 m	Deg
	Dir_metmast_10m	Direction at 10 m	Deg
	Wsp_OMS_160m	Cup wind speed at 160	m/s

		m at the light tower	
cov_10min_detrend		10-min covariances for turbulence parameters from the sonics	
	name	Name of the time series	
	vertical	Measurement height	m
	flux	Sonic heat flux	K m/s
	u_star3d	Sonic friction velocity	m/s
	L_3d	Sonic Obukhov length	m
caldata_200X_XX_20hz		20 Hz high frequency sonic measurements from a month period "200X_XX"	
	scan_id	Measurement ID number (1:12000)	
	Sonic_status_Xm	Status of the sonic at a "X" height	
	X_Xm	Longitudinal sonic wind speed	m/s
	Y_Xm	Transversal sonic wind speed	m/s
	Z_Xm	Vertical sonic wind speed	m/s
	T_Xm	Sonic temperature	deg. C
	Sonic_status_OMS_160m	Status of the light tower sonic at 160 m	
	X_OMS_160m	Longitudinal sonic wind speed at 160 m at the light tower	m/s
	Y_OMS_160m	Transversal sonic wind speed at 160 m at the light tower	m/s
	Z_OMS_160m	Vertical sonic wind speed at 160 m at the light tower	m/s
	T_OMS_160m	Sonic temperature at 160 m at the light tower	Deg. C

5 Conclusion and perspective

The 12MW project was successful in observing winds and turbulence profiles using wind lidar during the 6-month campaign at Horns Rev offshore wind farm in close collaboration between Risø DTU and DONG energy.

The observations proved to be of very high quality in the comparison analysis between offshore met-mast data and wind lidar data at one overlapping height (~ 60 m above sea level). This positive result enabled combining observations from 15 m up to 160 m at 8 heights. The wind profile thus obtained showed very interestingly that in some cases the surface boundary layer was shallower than 160 m. In other words, the mean wind observed at levels from around 100 m and up are NOT predicted well using the logarithmic wind profile in stable conditions.

The campaigns at Høvsøre using lidar up to 300 m and comparing met-mast data and lidar data at six overlapping heights again showed a remarkably good correlation. The extended wind profile using a combination of met-mast data at lower heights and lidar data at higher levels provided a unique wind profile with unprecedented detail. The results again demonstrated that also over land the upper part of the wind profile cannot be described by the surface layer logarithmic wind profile. As alternative, it was demonstrated that the boundary layer height is needed as scaling parameter.

Several other very interesting findings were obtained, e.g. a new formula for normalization for ocean roughness when presenting offshore wind profiles into stability classes was developed. This elegantly enabled the first results of the work. Another finding is the turbulence observed by lidar up to very high levels. For the first time turbulence profiles offshore up to 160 m and on land up to 300 m were obtained and analyzed. The theoretical physical background on observing turbulence from mast-data ('point') and lidar (volume) was detailed and presented. Furthermore from spectral analysis the dominant length scale was tested in comparison to other mixing length scales. The results showed a good correspondence. Finally should be mentioned the interesting results on observing the boundary layer height using ceilometer and comparing to theories and as well use the information for successful scaling of the wind profiles in the entire boundary layer!

The scientific results are published widely, yet it is too early to know the entire value of the **12MW** project. We would like mention the excellent Ph.D. thesis of Dr. Alfredo Peña as a result of the project. Also we would like to mention our new international engagement in the EU-Norsewind project http://www.norsewind.eu in which our state-of-the-art expertise are used in collaboration with international science and industry partners on observing offshore winds at high levels for the Baltic Sea, North Sea and Irish Sea in a 2-year campaign and analyze winds and turbulence for a Wind Atlas.

5.1 Perspective

Offshore wind farming appears to be THE renewable energy solution in the next decade that will provide society with MOST clean energy. The knowledge on how multi-farms – mega-clusters – of wind farms will interact with the marine atmosphere is UNKNOWN. Simplified theories definitely should be verified by observational evidence. Several unknowns and (poor) model parametrizations not justified in this specific environment are what we currently have. A mission to observe this relatively unknown environment seems RELEVANT – a mission far beyond individual developers and clearly a strategic research topic for society!

6 Publication

6.1 Referred Journals

Mann, J., **Courtney, M.,** Bingöl, F., **Peña, A.,** and Wagner, R. (2009) Lidar scanning of momentum flux in and above the surface layer, Manuscript in preparation.

Peña, A., Gryning, S.-E., and **Hasager, C.B** (2009) Comparing mixing-length models of the diabatic wind profile over homogenous terrain, *Theo. Appl. Climatol.,* in review.

Peña, A., Gryning, S.-E., Mann, J., and **Hasager, C.B** (2008) Length scales of the neutral wind profile over homogeneous terrain, *J. Appl. Meteor. Climatol*., in review.

Peña, A., Gryning, S.-E., and **Hasager, C.B** (2008) Measurements and modelling of the wind speed profile in the marine atmospheric boundary layer, *Bound.-Layer Meteorol.,* **129**, 479−495.

Peña, A. and **Gryning, S.-E.** (2008) Charnock's roughness length model and non-dimensional wind profiles over the sea, *Bound.-Layer Meteorol.,* 128, 191−203.

Hasager, C.B., Peña, A., Christiansen, M.B., Astrup, P., Nielsen, M., Monaldo, F., Thompson, D., and Nielsen, P. (2008) Remote sensing observation used in offshore wind energy, *IEEE J. Selected Topics in Appl. Earth Observations and Remote Sens.*, 1, 67−79.

Peña, A., Hasager, C.B, Gryning, S.-E., Courtney, M., Antoniou, I., and **Mikkelsen, T.** (2009) Offshore wind profiling using light detection and ranging measurements, *Wind Energy*, 12, 105−124.

6.2 Reports

Hasager, C.B., Peña, A., Mikkelsen, T., Courtney, M., Antoniou, I., **Gryning, S.-E.**, Hansen, P., and **Sørensen, P.B**. (2007) 12MW Horns Rev experiment, Tech. Rep. Risø R-1506(EN), Roskilde

6.3 PhD thesis

Peña, A. (2009) Sensing the wind profile, Ph.D. thesis, Risø PhD-45(EN), ISBN 978-87-550-3709-0, Roskilde

6.4 Chapter Books

Hasager, C.B., Christiansen, M.B., **Peña, A**., Badger, J., Antoniou, I., Nielsen, M., Astrup, P., and **Courtney, M.** (2009) Advances in offshore wind resource estimation, Advances in Wind Energy Conversion Technology, S. Mathew and G. S. Philip, Eds., Springer-Verlag.

6.5 Conference proceedings paper with oral presentation

Peña, A., Gryning, S.-E., Hasager, C.B. and **Courtney, M.** (2009) Extending the wind profile much higher than the surface layer, Proc. of the European Wind Energy Conf., Marseille

Peña, A., Gryning, S.-E., and **Hasager, C.B**. (2007) Lidar observations of offshore winds at future wind turbine operating heights, Proc. of the European Offshore Wind Conference, Berlin

Peña, A., Hasager, C.B., Gryning, S.-E., Courtney, M., Antoniou, I., **Mikkelsen, T.,** and **Sørensen P.** (2007) Offshore winds using remote sensing techniques, *J. Phys: Conf. Proc*. 75, 012038 (11 pp)

6.6 Oral presentations with extended abstracts

Peña, A. (2008) Wind speed distributions in neutral atmospheres over homogeneous terrain, Proc. of the 4th PhD seminar on Wind Energy in Europe, Magdeburg

6.7 Poster presentations with conference paper

Ohsawa, T., Kataoka, A., Heinemann, D., Lange, B., **Peña, A.,** and **Hasager, C.B.** (2007) Derivation and application of an empirical equation to estimate hub-height wind speed from sea surface wind speed, Proc. of the European Offshore Wind Conference, Berlin

Peña, A., Hasager, C.B., Gryning, S.-E., Courtney, M., Antoniou, I., **Mikkelsen, T.,** and **Sørensen P.** (2007) On the study of wind energy at great heights using remote sensing techniques, Proc. of the European Wind Energy Conference, Milan

6.8 Oral presentations in workshops with published slides

Peña, A., Hasager, C.B., Gryning, S.-E., Mikkelsen, T., Antoniou, I., **Courtney, M**., and **Sørensen, P.** (2007) Offshore winds using remote sensing techniques, Rep. of the 51st IEA topical expert meeting: State of the art of remote wind speed sensing techniques using sodar, lidar and satellites, Roskilde

6.9 Oral presentations in conferences

Peña, A. (2007) Non-dimensional wind profiles over the sea, 3rd PhD seminar on Wind Energy in Europe, Oral presentation, Pamplona

Hasager, C.B.(2009) **12 MW wind turbines** Presented at: EnergiForsk 2009. København (DK), 18 Jun., 2009

6.10 Poster presentations in conferences

Hasager, C.B., Peña, A., Gryning, S.-E., Mikkelsen, T., and **Courtney, M.** (2009) Wind profiles for large wind turbines, European Geosciences Union, general assembly, Poster presentation, Vienna

Peña, A., Hasager, C.B., Gryning, S.-E., Courtney, M., Antoniou, I., **Mikkelsen, T.,** and **Sørensen P.** (2007) Evaluation of the offshore wind resource using lidar measurements, European Geosciences Union, general assembly, Poster presentation, Viena

Peña, A. (2006) Study of wind energy at great heights using remote sensing techniques, 2nd PhD seminar on Wind Energy in Europe, Poster presentation, Roskilde

7 References

Blackadar, A.K. (1962) The vertical distribution of wind and turbulent exchange in a neutral atmosphere. *J. Geophys. Res.,* 67, 3096−3102

Businger, J. A., Wyngaard, J. C., Izumi, Y., and Bradley, E. F. (1971) Flux-profile relationships in the atmospheric surface layer. *J. Atmos. Sci.*, 28, 181–189.

Eberhard, W.L, R. Cupp and H R. Healy(1989) Doppler Lidar Measurement of Profiles of Turbulence and Momentum Flux. J. Atmos. Oceanic Tech. Vol. 6, pp 809- 819.

Gryning, S.-E., Batchvarova, E., Brümmer, B., Jørgensen, H., and Larsen, S. (2007) On the extension of the wind profile over homogeneous terrain beyond the surface layer. Bound.-Layer Meteor., 124, 251−268.

Hasager, C.B., Peña, A., Mikkelsen, T., Courtney, M., Antoniou, I., Gryning, S.-E., Hansen, P., and Sørensen, P.B. (2007) 12MW Horns Rev experiment, Tech. Rep. Risø R-1506(EN), Roskilde

Högström, U., 1988: Non-dimensional wind and temperature profiles in the atmospheric surface layer: a re-evaluation. *Bound.-Layer Meteorol.*, 42, 55–78.

Jørgensen, H.E., Mikkelsen, T., Gryning, S.-E., Larsen, S., Astrup, P., and Sørensen, P.E. (2008) Measurements from Høvsøre met mast. Tech. Rep. Risø R-1592(EN), Roskilde

Kaimal, J. C., Wyngaard, J. C., Izumi, Y., and Cote, O. R. (1972) Spectral characteristics of surface-layer turbulence. *Quart. J. Roy. Meteor. Soc.*, 98, 563−589.

Lettau, H. (1950) A re-examination of the Leipzig wind profile considering some relations between wind and turbulence in the frictional layer. *Tellus*, 2, 125−129.

Lettau, H. H. (1962) Theoretical wind spirals in the boundary layer of a barotropic atmosphere. *Beitr. Phys. Atmos.*, 35, 195−212.

Mann, J. (1994) The spatial structure of neutral atmospheric surface-layer turbulence. *J. Fluid Mech.,* 273, 141−168.

Panofsky, H. A. (1973) Tower micrometeorology. Workshop on Micrometeorology, D. A. Haugen, Ed., American Meteorology Society, 151−176.

Peña, A., Gryning, S.-E., Mann, J., and Hasager, C.B (2008) Length scales of the neutral wind profile over homogeneous terrain, *J. Appl. Meteor. Climatol*., in review.

Peña, A., Hasager, C.B, Gryning, S.-E., Courtney, M., Antoniou, I., and Mikkelsen, T. (2009a) Offshore wind profiling using light detection and ranging measurements, *Wind Energy*, 12, 105−124.

Peña, A., Gryning, S.-E., and Hasager, C.B (2009b) Comparing mixing-length models of the diabatic wind profile over homogenous terrain, *Theo. Appl. Climatol.,* in review.

Risø DTU is the National Laboratory for Sustainable Energy. Our research focuses on development of energy technologies and systems with minimal effect on climate, and contributes to innovation, education and policy. Risø has large experimental facilities and interdisciplinary research environments, and includes the national centre for nuclear technologies.

Risø DTU
National Laboratory for Sustainable Energy
Technical University of Denmark

Frederiksborgvej 399
PO Box 49
DK-4000 Roskilde
Denmark
Phone +45 4677 4677
Fax +45 4677 5688

www.risoe.dtu.dk